Design Propozal:
Mach-Zehnder Interferometer

1. Introduction

Silicon photonics has established itself as a pivotal technology for high-density integrated optics, driven largely by its compatibility with the mature complementary metal-oxide-semiconductor (CMOS) manufacturing infrastructure (Bogaerts & Chrostowski, 2018). This platform typically utilizes Silicon-on-Insulator (SOI) wafers, where the high refractive index contrast between the silicon core and the silicon dioxide cladding enables the tight confinement of light within sub-micron waveguides (Bryant et al., 2025). This confinement capability allows for the creation of compact photonic integrated circuits (PICs) with small bend radii, essential for scaling optical networks and computing systems.

A fundamental component within these circuits is the Mach-Zehnder Interferometer (MZI). The MZI serves as a versatile building block for manipulating the phase and amplitude of optical signals (Sun et al., 2022). Its operational principle—based on the interference of split optical paths—has enabled a wide array of applications, ranging from high-speed electro-optic modulation and optical switching to highly sensitive environmental sensing (Sultan et al., 2023; Sun et al., 2022). This report explores the design and theoretical underpinnings of MZI devices based on strip silicon waveguides, examining how geometric parameters and path asymmetries influence spectral performance.

2. Theory

2.1 Operating Principle

The operation of an integrated MZI relies on the splitting and subsequent recombination of a coherent optical signal. Light entering the device is divided into two separate arms, typically via a directional coupler or a multimode interference (MMI) splitter. As the light propagates through these arms, it accumulates a phase shift ϕ determined by the waveguide's effective refractive index n_{eff} and the physical length L of the path (Sun et al., 2022).

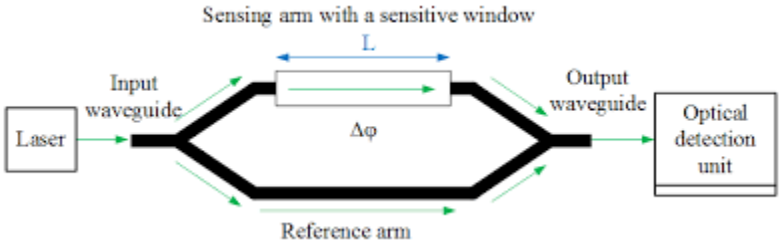

In an unbalanced MZI configuration, a physical path length difference ΔL is introduced between the two arms. The resulting phase difference $\Delta\phi$ between the propagating signals is wavelength-dependent and is given by:

$$\Delta\phi(\lambda) = \frac{2\pi n_{eff}(\lambda)\Delta L}{\lambda}$$

where λ is the operating wavelength in vacuum (Sun et al., 2022).

2.2 Transmission Characteristics

When the optical signals from the two arms recombine, they interfere either constructively or destructively depending on their relative phase difference. For an ideal lossless MZI with a 50:50 splitting ratio, the normalized output intensity I_{out} follows a sinusoidal transfer function described by:

$$I_{out} = \frac{1}{2}[1 + \cos(\Delta\phi(\lambda))]$$

This interference mechanism results in a periodic spectral response characterized by transmission maxima (constructive interference) and minima (destructive interference) (Sun et al., 2022).

2.3 Free Spectral Range and Group Index

A critical performance metric for interferometric devices is the Free Spectral Range (FSR), defined as the wavelength spacing between consecutive transmission peaks. The FSR is inversely proportional to the path length imbalance and the group index n_g of the waveguide (Bryant et al., 2025). The relationship is expressed as:

$$FSR \approx \frac{\lambda^2}{n_g \Delta L}$$

The group index n_g accounts for the dispersive nature of the waveguide medium, incorporating both material and waveguide dispersion effects. It is derived from the effective index using the following relation (Dulkeith et al., 2006):

$$n_g(\lambda) = n_{eff}(\lambda) - \lambda\frac{dn_{eff}}{d\lambda}$$

Accurate modeling of n_{eff} and n_g is essential for predicting the MZI's spectral behavior, particularly for applications requiring precise wavelength filtering or modulation (Bryant et al., 2025).

3. Modeling and Simulations:

3.1 Waveguide Modeling:

Here we consider a silicon-on-insulator (SOI) waveguide which consists of a low-loss silicon rectangle within a silicon dioxide layer. The standard height of the silicon box is set to 220 nm as per industry standards. The width of the waveguide can be varied, however we selected a standard width of 500 nm as this allows us to operate within the single-mode regime at low loss. This arises from a tradeoff between sidewall scattering and single-modedness. For smaller

waveguides a larger portion of the field interacts with the sidewall leading to higher scattering while larger waveguides lead to multiple modes being supported within the waveguide.

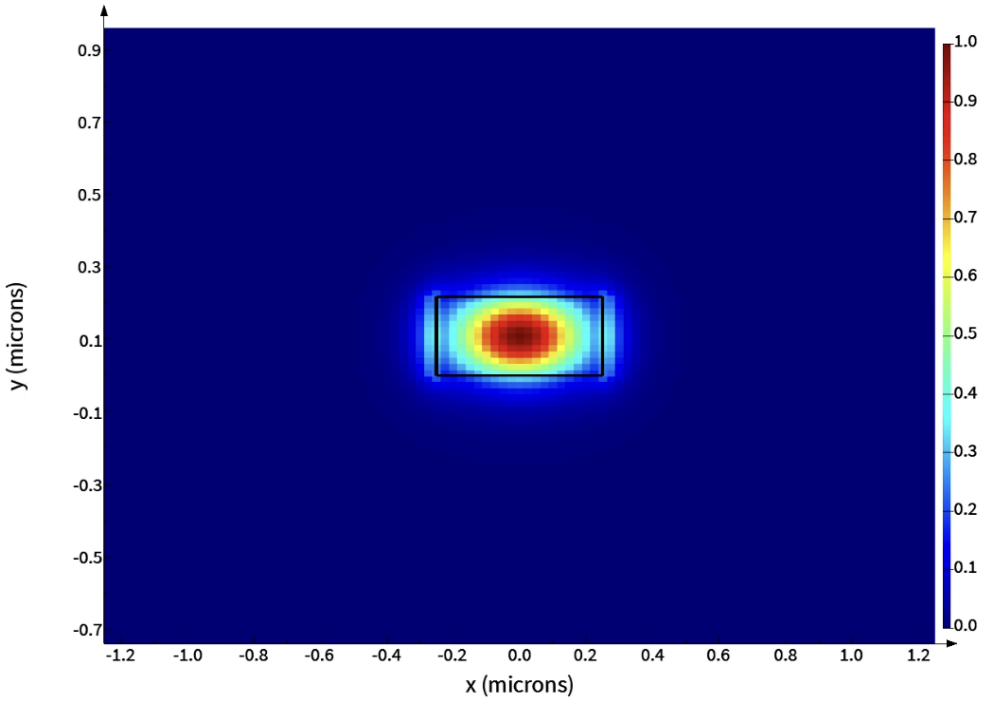

Figure 2: $|E|^2$ mode for a 220 x 500 nm SOI waveguide.

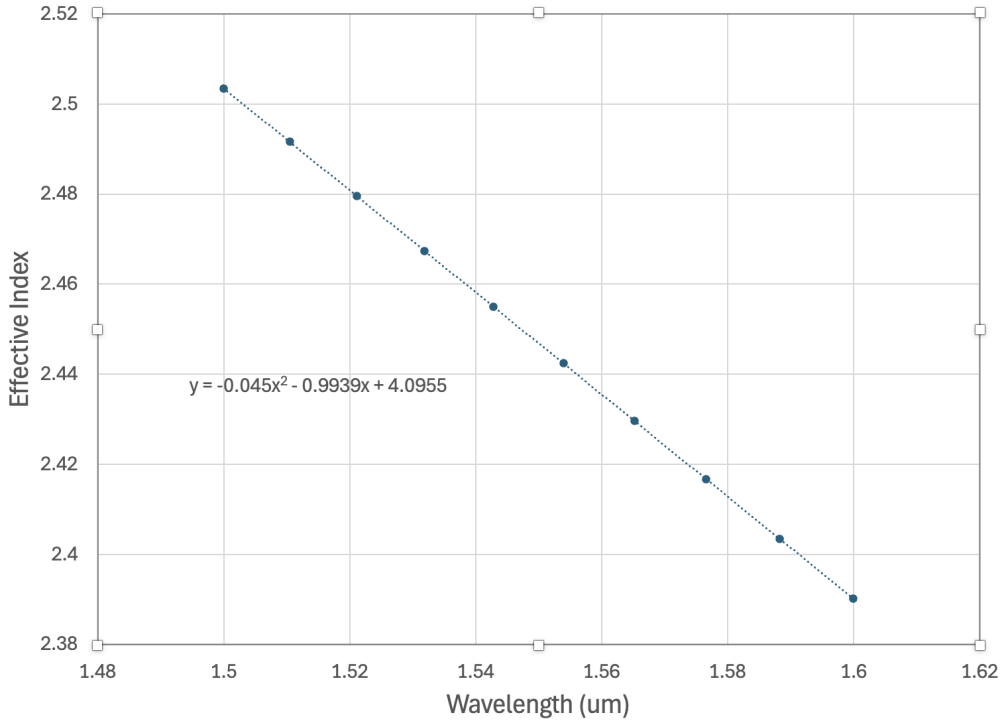

Figure 3: Effective index for a 220 x 500 nm SOI waveguide vs wavelength.

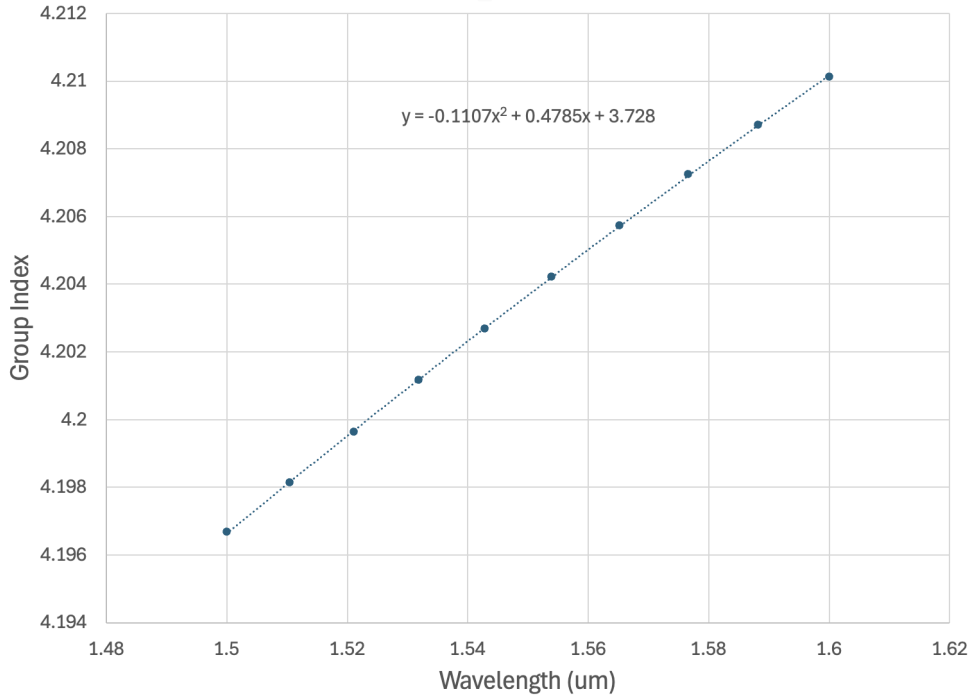

Figure 4: Group index for a 220 x 500 nm SOI waveguide vs wavelength.

Based on the polynomial fits to our simulations we are able to extract:

$$n_{eff} = -0.045\lambda^2 - 0.9939\lambda + 4.0955$$

$$n_g = -0.1107\lambda^2 + 0.4785\lambda + 3.728$$

3.2 Mach-Zehnder Interferometer Modeling:

The model for MZI, shown in Figure 5, included an input grating , y-splitter, two waveguides , another y-splitter and an output grating.

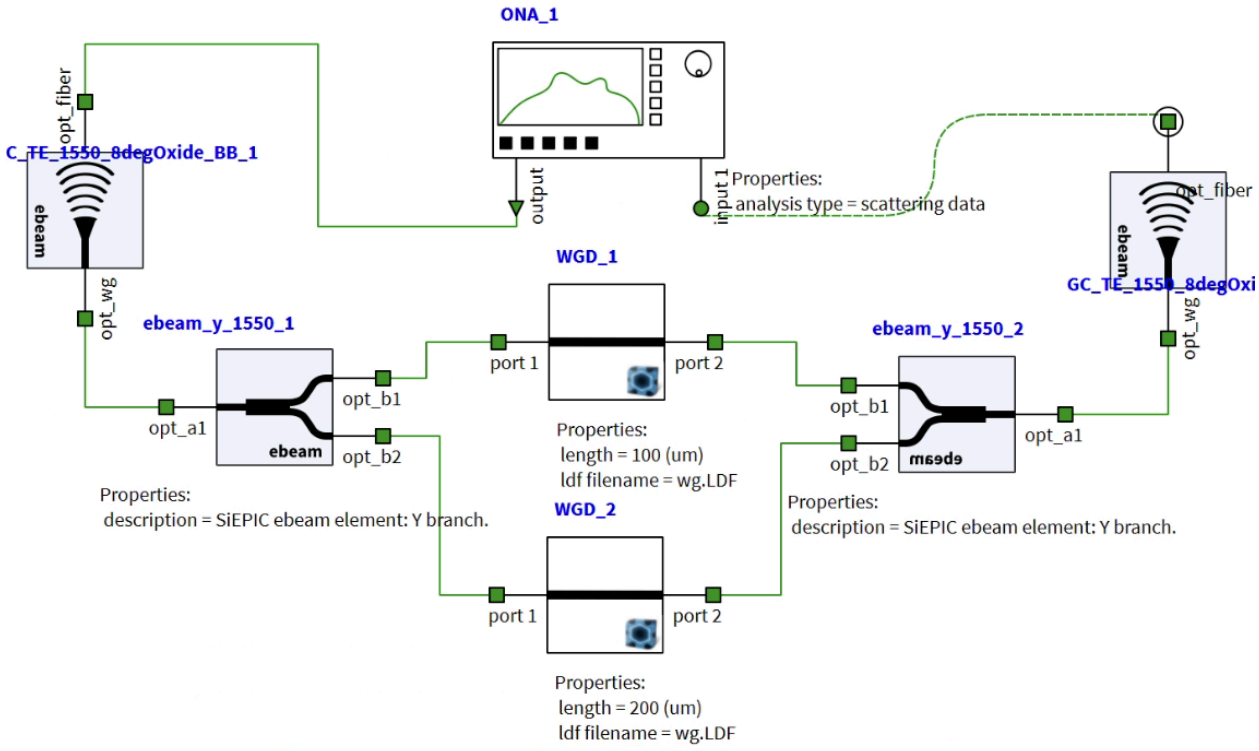

Figure 5: Lumerical Interconnect model for our MZI.

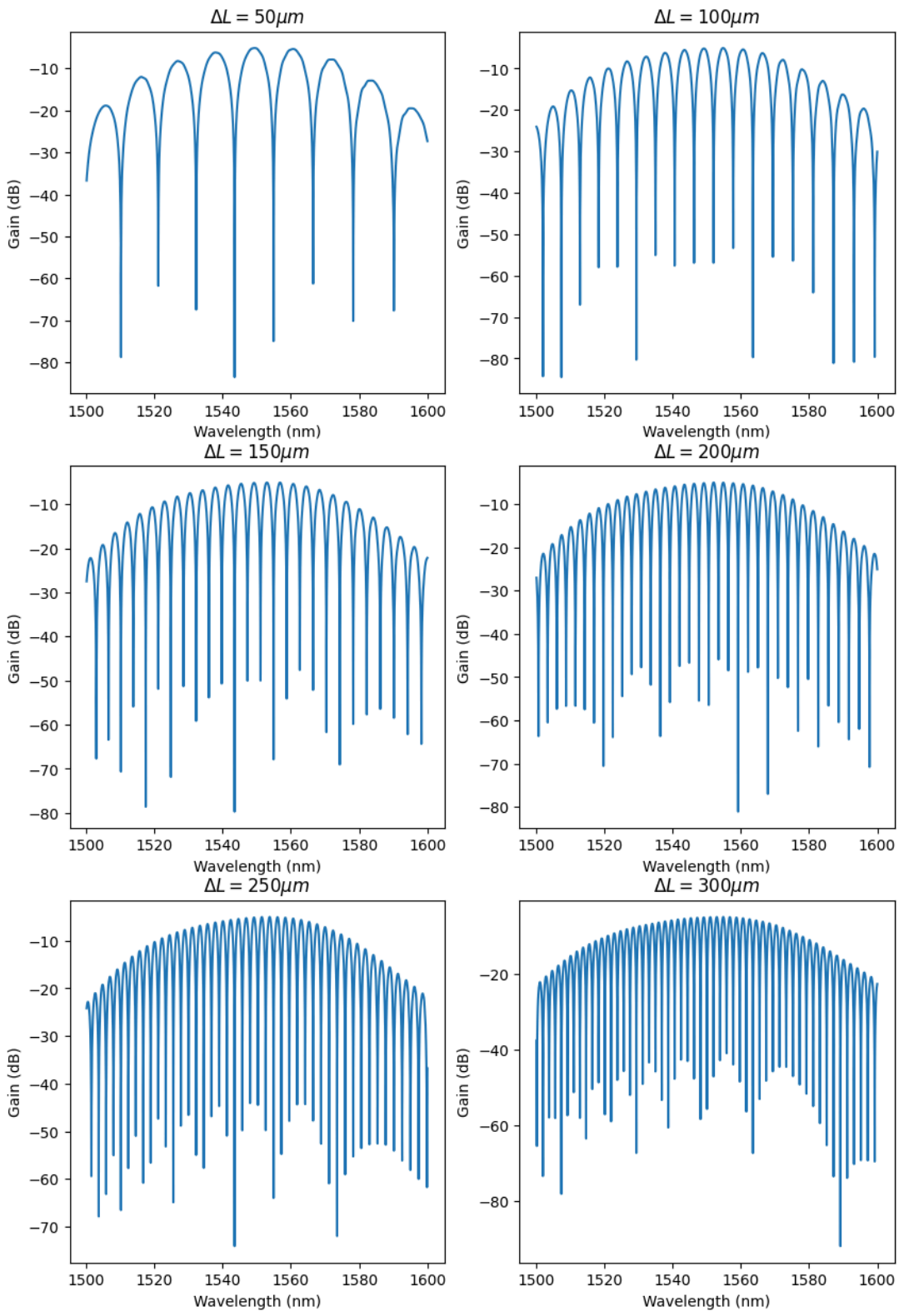

Figure 6: MZI response function vs wavelength for a variety of imbalanced lengths $\Delta L = 50, 100, 150, 200, 250, 300\ \mu m$.

References

Bogaerts, W., & Chrostowski, L. (2018). Silicon Photonics Circuit Design: Methods, Tools and Challenges. *Laser & Photonics Reviews*, 12. https://doi.org/10.1002/lpor.201700237

Bryant, K., Hokkanen, A., Shahwar, D., Harjanne, M., Salmi, A., & Aalto, T. (2025). Zero Birefringence and Zero Birefringence Dispersion in 3 μm-Thick Silicon-on-Insulator Waveguides. *Journal of Lightwave Technology*, 43, 747–756. https://doi.org/10.1109/jlt.2024.3467707

Dulkeith, E., Xia, F., Schares, L., Green, W. M. J., & Vlasov, Y. A. (2006). Group index and group velocity dispersion in silicon-on-insulator photonic wires. *Optics Express*, 14, 3853. https://doi.org/10.1364/oe.14.003853

Sultan, A., Sabry, Y. M., Samir, A., & El-Aasser, M. A. (2023). Mirror-terminated Mach-Zehnder interferometer based on SiNOI slot and strip waveguides for sensing applications using visible light. *Frontiers in Nanotechnology*, 5. https://doi.org/10.3389/fnano.2023.1121537

Sun, H., Qiao, Q., Guan, Q., & Zhou, G. (2022). Silicon Photonic Phase Shifters and Their Applications: A Review. *Micromachines*, 13, 1509. https://doi.org/10.3390/mi13091509